NASA Technical Memorandum 83213

NASA-TM-83213 19820004267

THE EFFECT OF RESIN ON THE IMPACT DAMAGE TOLERANCE OF GRAPHITE-EPOXY LAMINATES

JERRY G. WILLIAMS AND MARVIN D. RHODES

OCTOBER 1981

National Aeronautics and Space Administration

Langley Research Center
Hampton, Virginia 23665

INTRODUCTION

Experimental studies have shown that the compression strength of graphite-epoxy structures may be seriously degraded by impact damage (ref. 1 and 2). In these studies, specimen damage caused by impact resulted in strength reductions of 60 to 70 percent compared to undamaged specimens. The failure mode frequently involved delamination associated with fracture of the matrix. It was postulated, therefore, that improvements in the compression strength of damaged graphite-epoxy panels could be obtained by "toughening" the resin matrix material. Several investigators have proposed additives and chemical formulations to toughen resin systems and several approaches are reported in references 3-7. The evaluation of these approaches is commonly based on the energy absorbed during impact and little effort has been conducted to identify the matrix properties required to reduce the size of damage and to retain high compression strength following local impact damage.

In the investigation reported herein, the damage characteristics including the effect of damage on compression strength were evaluated for 24 different resin systems, 23 of which incorporated resin toughening techniques. Candidate materials were supplied in prepreg form by seven resin manufacturers who were solicited to supply formulations which they anticipated might provide improved damage tolerance. Materials were not competitively submitted for the purpose of selecting a best material, but were voluntarily provided to study what improvements in damage tolerance various resin modifications might make. A few of the resin systems are commercially available, however, many are experimental formulations. Suppliers were instructed to ignore other important considerations such as processing and environmental factors and to concentrate

only on modifications that would improve damage tolerance. Rigidite 5208[1] resin system was selected as the baseline control resin because it is a widely used system and its damage tolerance characteristics have been documented in several prior studies (ref. 1, 2, 8). To eliminate the fiber as a variable, all candidate resins were combined with unidirectional Thornel 300[2] graphite fiber to form a prepreg tape. The Douglas Aircraft Company fabricated the test specimens used in the present study and also conducted an independent complementary investigation reported in reference 9.

The present paper describes the results of tests conducted to measure the extent of damage resulting from projectile impact and the effect of impact on compression strength of the different composite materials systems. The improvements achieved using these currently available and newly developed experimental resin formulations are discussed. Resin properties common to material systems exhibiting improved damage tolerance are identified. Current test methods designed to assess damage tolerance are reviewed, and a new test method which simulates the local deformations sustained by a laminate during impact is described.

Identification of commercial products in this report is used to adequately describe the test materials. Neither the identification of these commercial products nor the results of the investigation published herein constitute official endorsement, expressed or implied, of any such product by NASA.

---

[1]Rigidite 5208: Trade name of Narmco Materials Corporation.
[2]Thornel 300: Trademark of Union Carbide Corporation.

MATERIALS AND SPECIMENS

Resin Materials

Five approaches were identified by the suppliers as methods used in their products to provide improved resin toughness, however, additional approaches may also have been used. Identified approaches include the use of different base epoxy materials, different curing agents, elastomeric additives, thermoplastic additives, and vinyl modifiers. The resin materials evaluated are described in table I. The resin identification is that used by the material supplier. Resins commercially available in prepreg form are denoted by their current product designation and specially prepared experimental prepreg formulations have an X prefix. The generic chemistry, cure temperatures, and the neat resin mechanical properties shown in table I were provided by the material suppliers. Test techniques used to measure mechanical properties were not identified and may vary between material suppliers.

Tensile stress-strain curves for some of the neat resin materials were also supplied by the resin manufacturers and available data are presented in figure 1. The curve for material 1 (5208) is shown for comparison. Results from a preliminary study of the two material systems reported in reference 10 indicate that to achieve high compression strength in the presence of impact damage the neat resin should have a higher ultimate tensile stress and strain than that of material 1. Nearly all of the resin systems evaluated have higher ultimate strains than material 1, however, the ultimate tensile strength of several systems is about the same (table I). All of the curves shown, except that for material 1, are highly nonlinear and exhibit ductility.

Composite Material Properties

Unidirectional laminate properties for specimens constructed of the various resin materials are tabulated in table II. Property measurements were made by the Douglas Aircraft Company (ref. 9) using 6-ply 0^{o} sandwich beam specimens and 16-ply, 0^{o} short beam shear specimens. Tensile strength and modulus values for all materials are similar which is to be expected since these laminate properties are filament controlled. Compression and short beam shear strengths, however, are influenced more by the matrix properties and some of these materials have substantially lower strengths than the values recorded for material 1. For example, the compression strength for material 19 is only .48 GPa compared to 1.45 GPa for material 1. These low compression strengths could be a result of filament microbuckling caused by low values for the resin shear modulus. A discussion of the effect of resin modulus on microbuckling may be found in reference 11. Resin shear modulus values were unavailable for the matrix materials. However, for an isotropic matrix, the shear modulus should vary in a manner similar to the tension modulus. Comparison of data in tables I and II show that laminates with low compression strengths are fabricated from resins with low values of tensile modulus.

Specimens

The specimens evaluated in this investigation were 48 ply orthotropic laminates with the following ply orientation: $[\pm 45/0_2/\pm 45/0_2/\pm 45/0/90]_{2S}$. The orientation and stacking sequence were selected because the laminate has elastic properties typical of those required in heavily loaded aircraft wing structures and considerable impact data on the laminate were available. The laminates were fabricated using conventional techniques and autoclave cured according to

the procedures supplied by the resin manufacturers. All laminates were inspected ultrasonically to assure freedom from disbonds or foreign inclusions, and evaluated to determine resin and void content. Additional details concerning the specimens are available in reference 9. The test specimens were cut from cured laminates using diamond-impregnated tooling and the panels used for compression tests were ground flat and parallel on the ends to be loaded.

EXPERIMENTAL PROCEDURE

Several techniques were used to assess the impact damage tolerance of the composite resin systems. These techniques involved both standard test methods as well as a new method developed specifically for this investigation.

Measurement of the Extent of Impact Damage

The size and character of local damage were determined following impact by a 1.27 cm diameter aluminum sphere striking a 12.7 cm square plate at normal incidence. A nominal impact velocity of 100 m/s was selected based on the results of previous tests conducted on material 1 (reference 2) in which this impact condition created substantial interior laminate damage and resulted in 60 to 70 percent reductions in the laminate compression strength.

Following impact, each test specimen was inspected visually and ultrasonically, and then cross-sectioned normal to the direction of the 0^{o} fibers through the impact site using a diamond-impregnated saw. All specimens were examined with an optical microscope and selected specimens were inspected with a scanning electron microscope to study the interior fracture surface.

Impact Under Compression Load

Specimens approximately 25.4 cm long and 12.7 cm wide were subjected to impact at the specimen center while under static compression load. A photograph of a typical specimen is shown in figure 2(a). The projectile used was a 1.27 cm diameter aluminum sphere and impact was at normal incidence to the specimen. The specimens were simply supported along the sides by adjustable edge supports and clamped on the top and bottom ends where the load was applied. Some of the specimens sustained local damage and continued to carry load following impact while others failed catastrophically. Specimens which continued to carry load were inspected and subsequently loaded to failure to determine the residual strength.

Multi-Span Beam Shear Test

Severe local deformations develop in a composite laminate due to impact (see ref. 10). For a 1.27 cm diameter aluminum sphere impacting at 91 m/s, a deformation amplitude of approximately 1 mm and half-wavelength of approximately 2.54 cm was recorded for a 48ply orthotropic laminate (see Sketch A). This deformation creates high interlaminar shear stresses which may result in local delamination.

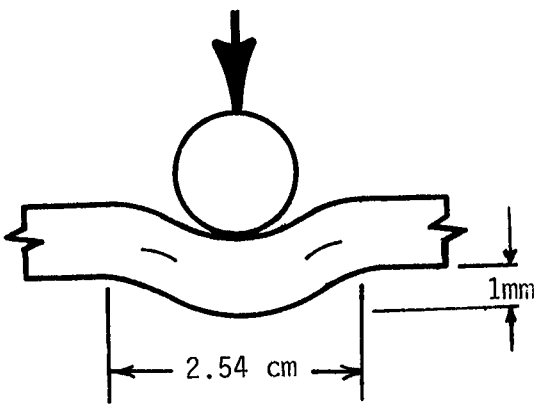

Sketch A

The multi-span beam shear test apparatus shown in figure 2(b) was developed to simulate in two-dimensions the laminate deformations resulting from impact. Steel half cylinders 1.27 cm in diameter were used to provide line loads across the width of a 2.54 cm wide by 10.2 cm long beam specimen. The half cylinders attach to two sets of steel blocks which when loaded imposed a uniform displacement to the two sets of line loads. The 2.54 cm distance between line loads provided a span-to-thickness ratio of four for the 48-ply orthotropic laminate. Uniformly spaced vertical lines were scribed on the edge of the specimen and accented with white paint to aid in visually locating the region of the initial interlaminar shear failure.

A multiple load set consisting of five or more line loads is necessary to simulate in the center bay the boundary conditions characteristics of impact. A line load set consisting of three line loads on the top and four on the bottom was selected for the test configuration. The reaction loads obtained from a finite element analysis (normalized to the highest value) and shear diagram for this configuration are shown in Sketch B. The magnitude of shear

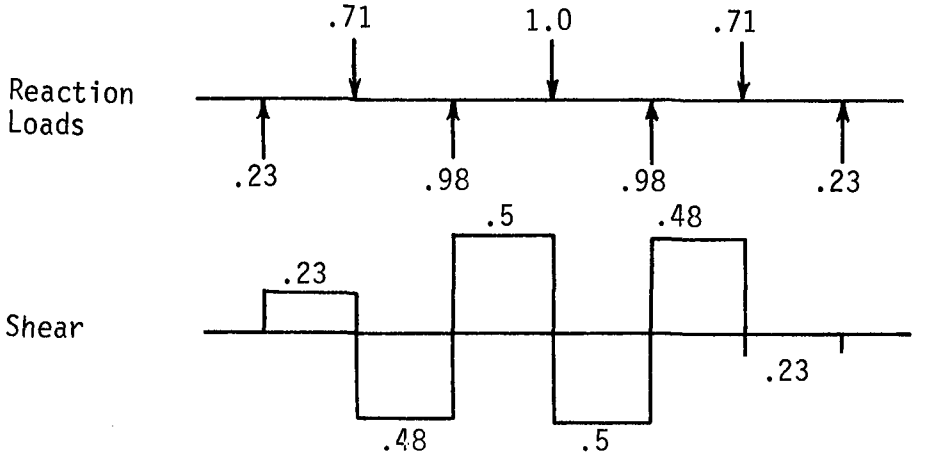

Sketch B

in the center region is reduced by over 50 percent in the end bays. Development of the highest shear stress in the center bay causes interlaminar shear failure to initiate in this region. Beam specimens of each of the material systems were tested in this manner.

RESULTS AND DISCUSSION

Extent of Impact Damage

The damage in each of the resin material systems resulting from projectile impact is given in table III. The damage was evaluated by visual inspection of the surface and ultrasonic C-scan inspection of the laminate interior. All of the systems had a smaller interior damage region than material 1 (5208) as determined by C-scan inspection, and all except material 14 had less visible damage on the specimen surface. Although the impact test condition was adequate to create interior damage in each material system evaluated, several of the systems had interior damage that was not visually detectable on the specimen surface. All laminates that had visually detectable surface damage had a larger damage region on the back side of the specimen than on the contact side.

Photographs showing damage in the laminate cross-section and areal damage for two material systems are shown in figure 3. These material systems were selected for presentation because, as seen in table III, they represented systems near the extremes of the damage range. Material 1 shows extensive delamination and intraply fracture extending throughout the cross-section while material 19 has only local fracture of one or two plies in the impact zone without further evidence of interior damage. The difference in affected areas of these two materials as indicated by the C-scan is significant. Material 19 also has no visible damage on the surface while material 1 has extensive surface cracking and delamination. The local surface discoloration on the specimens is due to

spallation of a brittle lacquer coating painted on the surface prior to impact. The use of brittle lacquer as a damage detection technique is reported in reference 12.

C-scan results from Gardner impact tests reported in reference 9 for materials 1 and 19 are shown in figure 4a and a graph denoting the damaged area as a function of impact energy level for most of the materials evaluated is shown in figure 4b. These results were obtained on 8 ply quasi-isotropic laminates. There is considerable difference in the size of the C-scan damage region for these materials. Note from the graph that several of the materials consistently have lower damage area for each of the three impact energy levels. Since each data point represents a single test specimen, minor shifts in the relative ranking of the three different energy conditions are not considered significant.

The Gardner impact results from ref. 9 are compared in summary form in figure 5 with results from spherical projectile impact tests conducted in the present investigation (table III). The damage area as determined by C-scan inspection is shown as a function of impact energy for both test methods. Due to the large range of the C-scan area parameter, Gardner impact data from figure 4b are plotted only for material 1. Using material 1 as a baseline, the number of material systems that had a 50% improvement over material 1 (C-scan damage area of 50% or less) are indicated on figure 5. Also indicated on the figure by filled symbols are 5 materials (materials 3, 11, 12, 17 & 19) that indicated substantial improvement over material 1 in both the Gardner and ball impact tests and in compression loaded impact tests to be discussed subsequently.

The 48 ply laminates that were damaged by impact and cross-sectioned to evaluate the damage region were also examined microscopically. The results of

this study are reported in reference 13 and highlights of this investigation are discussed below. As noted in table I, many of the systems evaluated had elastomeric additives. The prominence of elastomeric modifiers was evident in the fracture surface of some of the cross-sections and typical examples are shown in figure 6. The most common evidence of elastomers was the formation of "pits" within the resin such as shown for material 15 in figure 6a. These pits are an indication of regions where elastomeric particles are present in the matrix. Another sign of elastomeric additives was the formation of resin "hairs" such as shown for material 21 in figure 6b. The fracture surfaces of some of the resin systems known to include elastomeric additives (table I), however, did not have the characteristic pits or hairy features. For example, material 5 in the neat resin form has been shown to have clearly defined pits in the fracture surface. The fracture surface of the impact damaged specimens, however, failed to reveal such evidence and extensive evaluation of the specimen even outside the damage zone failed to reveal the characteristic resin pits. The apparent change in morphology is believed due to processing. There was no attempt to optimize the cure cycle during laminate fabrication, and it is evident from results of tests reported in reference 9 on material 1 that cure cycle can have a dramatic effect on impact initiated damage. It is unclear what effect resin morphology may have on the character of impact damage created in elastomer modified systems such as material 5.

Microscopic examination of the fracture surface (reported in ref. 13) also indicated that those materials which had small areas of damage due to impact exhibited ductile resin behavior. Ductile behavior is characterized by a hackly appearance, and typical examples are presented in figure 7 for materials 12 and 19. By contrast, the failure surface for material 1 has a smooth, glassy appearance which is characteristic of a brittle material. Also, these

material systems exhibiting small damage areas indicated good fiber to matrix bonding. None of the fracture surfaces examined indicated evidence of fiber splitting in the cross-section or major fiber damage initiated by the projectile impact.

Impact Under Compression Load

The effect of projectile impact damage on the compressive failure strain of the 48 ply orthotropic plates for three of the matrix material systems (materials 1, 3, and 11) is shown in figure 8. The ordinates in figure 8 are axial strains measured on the specimen due to the applied compression load, and the abscissas are projectile impact velocities. The solid circular symbols (fig. 8a-8c) represent specimens that failed due to projectile impact while the open circles represent specimens that did not fail even though they may have incurred some local damage. A curve labeled "failure threshold" has been faired between the open and solid circular symbols of each set of data shown to represent a lower bound to the applied static compression strain that causes failure at a given velocity for the impact projectile used. Data points on the ordinate are failures of undamaged control specimens. These specimens failed after buckling at strains in excess of 0.008, and do not represent the ultimate static strength of the test laminates. The specimens that did not fail due to impact, as well as several that were damaged without an applied static load, were subsequently tested to determine the residual compression strains. These residual strain results are shown by the solid square symbols on figure 8. Every data point representing the residual strain is on or above the failure-threshold curve. This result suggests that impacting test specimens while under load is an effective method of establishing a lower bound for the

static compression strain of graphite-epoxy laminates damaged by low-velocity impact. A comparison of the failure-threshold curves for the three materials shown in figure 8(d) demonstrates clearly that the matrix material has considerable effect on impact damage tolerance. For example, the failure threshold strain for a 100 m/s impact condition is approximately 0.006 for material 3, 0.005 for material 11 and 0.003 for material 1.

Since most of the resin systems evaluated were experimental formulations supplied in small quantities, sufficient prepreg material was not available to fabricate enough specimens to determine a failure threshold curve for all of the material systems. Therefore, based on the damage tolerance improvements demonstrated with materials 3 and 11, a screening test was conducted in which candidate material systems were loaded to a strain of 0.005 and impacted at a velocity of 100 m/s. The test does not address the highest strain at which a material would have survived but simply separates the systems into pass and fail categories. Results of this screening test are shown in figure 9. Five of the materials (materials 3, 11, 12, 17 and 19) survived this severe impact condition, and the residual failure strain is indicated on figure 9. These test results represent a substantial improvement relative to the 0.003 failure threshold strain for material 1 at this impact condition. Although five materials passed the loaded impact screening test, each sustained limited local damage detectable by C-scan inspection. It is anticipated that some of the seventeen resin materials which failed the screening test would have passed a similar impact test conducted at a slightly reduced strain level.

The five materials that were able to sustain compression load with impact were also materials which had smaller damage areas in Gardner and ball impact tests than most of the other systems. All of these systems have a bisphenol A base (table I) but different modifiers and curing agents were used in the various

systems; materials 17 and 19 had elastomeric additives, materials 11 and 12 had thermoplastic additives, and material 3 had a vinyl modifier.

Failure Propagation Modes

Two modes of damage propagation, delamination and transverse shear crippling, are described in reference 10 for the failure of laminates loaded in compression. Damage in material 1 characteristically propagates in a delamination mode while the more damage tolerant material systems suppress delamination and fail at higher loads in a transverse shear crippling mode. The two modes of failure are illustrated in figure 10 by photographs of cross-sections through the damage regions of test specimens fabricated from materials 1 and 19. Delamination permits the local buckling of thin sublaminates which results in high tension peel stresses at the delamination boundary. The transverse shear failure mode is caused by shear instability in which the filaments buckle locally. For resin materials which suppress delamination, the compression strength of the impact damaged laminate is influenced by the shear modulus properties of the resin.

The initiation of failure in the transverse shear mode is illustrated in the photographs presented in figure 11. This specimen constructed of material 17 did not fail in the loaded impact screening test, but did exhibit a small horizontal surface crack in the vicinity of the impact (illustrated schematically in figure 11). To explore further the failure mode, the specimen was cross-sectioned and examined in a scanning electron microscope. The photographs of the cross-section reveal the damage extended through approximately half the thickness of the specimen. Examination at high magnification indicates the individual graphite filaments have failed in a short wavelength shear crippling mode.

Multi-Span Beam Shear

The 48 ply laminates of each of the 24 resin systems evaluated were tested in multi-span beam shear. For this test, the laminates were oriented with the 0^{o} plies across the width of the beam and the 90^{o} plies along the beam axis. A typical load deflection response for one test laminate is presented in figure 12 and photographs of the beam center bay region are shown on the right corresponding to selected points along the load deflection curve. At "A" the load-deflection curve is continuous, and the cross-section has no indication of interlaminar shear failure. The first evidence of erratic behavior in the load-deflection curve occurred at B and the accompanying photograph of the cross-section indicates a shear failure approximately 0.89 cm long has occurred near the beam mid-depth midway between the top and bottom line loads. This initial failure occurs in the region of maximum theoretical shear stress. At C additional locations of shear failures are evident and they are more extensive in size.

The load-displacement response for the five material systems that survived the impact screening test are compared in figure 13 with the response for material 1. Load and displacements have been normalized to the values for material 1 at first interlaminar shear fracture. The displacements at first interlaminar shear fracture for these five materials are approximately twice as large as that for material 1. The load and displacements for the first interlaminar shear fracture and the maximum load and corresponding displacement for all materials normalized to that of material 1 are listed in table 4. All of the materials tested except 17 and 19 followed the typical response defined in figure 12 in which the first interlaminar shear fracture was followed by a reduction in load. The load for materials 17 and 19 continued to increase and

exhibited no erratic load-deflection response following the first interlaminar shear fracture. The load-displacement curves for the remaining 18 materials fell between those of material 1 and materials 3, 11 and 12.

Resin Volume Fraction

The specimens of several of the damage tolerant materials (3, 12 and 19) had moderately high resin volume fractions and additional specimens with resin volume fractions nearer those generally used were fabricated to determine how resin volume fraction influenced test results. Results of this limited study are summarized in figure 14. High resin volume fractions are defined as laminates with 40 to 45 percent resin and low resin volume fractions as those with 35 to 40 percent resin.

The size of damage as indicated by C-scan measurements was larger for the low resin volume fraction specimens. For example, the C-scan damage measurement for the low resin specimen of material 19 (shown in figure 14(a)) was approximately twice as large as the measurement for the high volume fraction specimen. In addition, the failure strain of damaged specimens was consistently higher for panels with high volume fraction (see figure 14(b)). The low volume fraction specimen of material 12 even failed to pass the loaded impact test. The lower tolerance to damage with lower resin volume fraction was further corroborated in the multi-span beam shear test (figure 14(c)) in which the material 12 high resin volume fraction specimen has a substantially higher initial failure load.

The failure surface of the high and low volume fraction specimens were examined in a scanning electron microscope and results are reported in reference 13. The comparison for material 3 is shown in figure 14(d). There is more resin surrounding the fiber in the high volume fraction specimen and the rough

hackly surface suggests extensive resin plastic deformation. Fibers in the low volume fraction specimen are closely packed and there is less-evidence of plastic deformation. This evidence indicates that not only must the resin be capable of experiencing plastic deformation, but also there must be sufficient material available between fibers for a plastic zone to develop. A resin volume fraction on the order of 40 percent or greater (32 percent by weight) may be necessary to provide improved damage tolerance. To achieve high strength and stiffness, the resin volume fraction of graphite-epoxy composites are intentionally maintained low, however, these results suggest a compromise may be needed to achieve composites with high strength and stiffness and improved damage tolerance.

Discusson of Material Properties and Test Methods

Two current needs which limit the development of damage tolerant graphite-epoxy materials systems are (1) fundamental understanding of the importance of various material properties to damage tolerance and (2) reliable test methods adequate to assess during the development phase the damage tolerance of new material systems. The studies conducted in the present investigation along with complementary studies reported in references 9 and 13 provide insight into these two technology needs.

The mechanical property requirements for neat resin are discussed in reference 9. The results of this study indicate that modifications to the base epoxy matrix tensile properties have significant influence on the response of a laminate to impact. Based on the results of tests on materials 3, 11, and 12, it is evident that considerable improvements in impact properties can be expected with no significant loss in room temperature mechanical properties.

Neat resin ductility and high ultimate strength are necessary but not sufficient to ensure improvements in damage tolerance. Neat resin ultimate tensile strengths of greater than 69 MPa and strains at failure of greater than 4% were common to most systems that exhibited significant improvements in impact resistance. Very high neat resin failure strains, however, were not found to guarantee additional improvements. For example, material 23 with a 19% ultimate strain (table I) showed less improvement (table III) than other materials which had lower values. Although materials 17 and 19 also exhibited improved impact resistance, they had low compression strength (table II) in comparison to other materials such as 1, 3, 11 and 12. To ensure adequate laminate compression strength the resin should have a tensile modulus greater than 3.1 GPa and a shear modulus sufficiently high to prevent microbuckling.

Traditionally, the short beam shear test (ref. 14) has been used to evaluate composite materials and establish interlaminar shear strength. Resin material manufacturers have attempted to provide systems with high values of interlaminar shear strength based on short beam test results. The results reported in reference 9 for short beam shear tests as well as tests reported in reference 8 indicate that material 1 has one of the highest short beam strengths of any material evaluated. Short beam shear specimens frequently fail at the ends outside the loaded region and may be influenced by edge effects and surface roughness. The multi-span beam shear specimen, on the other hand, fails in the region of highest shear stress (near the specimen center) and test results correlate well with damage tolerance trends. To evaluate further the multi-span beam test, a comparison is made in figure 15 between the load at which interlaminar fracture first occurs (table IV) and the extent of damage indicated by C-scan in the 48 ply laminate impact tests (table III). The data indicates that the combination of limited damage area due to projectile impact and high

load associated with initial interlaminar failure are properties common to those materials showing improved damage tolerance when compared to material 1. The results from the multi-span beam tests, however, are preliminary; and additional evaluation of the method is required before it can be considered a reliable damage tolerance test.

Another test that may provide insight into composite damage tolerance is an interlaminar fracture test also known as the double-cantilever beam test. In this test, a laminate with an initial interlaminar crack is pulled apart and the load required to extend the crack is determined as a function of crack length. This test is of value because delamination is one of the principal failure modes in compression loaded composite structures. The type of specimen used to perform interlaminar fracture tests and interpretation of the results has been discussed in the literature (refs. 15 and 16). It is clear that for comparative purposes a test of this type can contribute to the development of new resin systems. For example, interlaminar fracture test results are reported in reference 17 and shown in figure 16 for two of the material systems studied in the present investigation. Material 1 which has a low failure threshold principally due to delamination propagation (ref. 12) requires considerably less load and fracture energy to propagate a crack than does material 3. Similar studies have also shown laminates fabricated from graphite fabric to be more damage tolerant and have greater toughness than corresponding laminates fabricated from prepreg tape (ref. 15 and 18). Although the minimum stress or fracture energy requirement for a damage tolerant resin remains undefined, studies are currently underway by a number of investigators to correlate interlaminar fracture and delamination propagation.

The Gardner impact and projectile impact are two methods for producing controlled impact damage in composite materials. Based on C-scan results

similar trends for the material systems evaluated were obtained using the two test methods. A controlled damage assessment test can serve as a discriminator between materials systems, however, it provides little insight into the reductions in strength which can be expected following impact damage.

The final evaluation of a material resistance to impact must be obtained using a test which measures the effect of damage on strength. The compression-loaded impact test is a candidate test for this purpose. Multiple experiments can be conducted to develop a failure threshold strain curve which defines a lower bound on the residual compression strength with local damage. Additional study, however, is needed to establish the effect of variations in projectile velocity; energy and impactor shape; specimen thickness; laminate stacking sequence and orthotropy; and specimen support boundary conditions. One problem with this test is that larger volumes of material are required than for traditional materials tests. It may be desirable, therefore, to conduct compression loaded impact tests only after a candidate material has satisfactorily met minimum requirements established for other tests.

CONCLUDING REMARKS

Twenty-four different epoxy resin systems were experimentally evaluated by a variety of test techniques to identify materials which exhibit improved impact damage tolerance in composite laminates. Damage tolerance characteristics were evaluated based on the extent of damage incurred within a laminate due to local impact and on the ability of a laminate to retain compression strength under impact conditions. Most of the materials tested had a smaller interior damage region as determined by C-scan inspection and less damage on the specimen surface than a baseline control resin which is widely used and whose damage tolerance characteristics have been documented in prior studies. Several

material systems demonstrated substantial improvements in residual strength following impact compared to the baseline material. For example, 48 ply composite panels of five of the material systems were able to sustain 100 m/s impact by a 1.27 cm diameter aluminum projectile while statically loaded to strains of 0.005. Composite panels of the baseline control resin could only sustain similar impact conditions at static strains less than 0.003. Several techniques were identified by resin suppliers as approaches used to toughen their products including the use of different base epoxies and curing agents. Of the five materials which exhibited the highest tolerance to impact; two systems had elastomeric additives, two systems had thermoplastic additives, and one system had a vinyl modifier. In addition, bisphenol A was the base resin used in all five materials.

Evaluation of the test results provided insight into the requirements necessary for graphite-epoxy materials to exhibit improved damage tolerance characteristics. Examination of the neat resin mechanical properties indicates that the tensile performance of the resin has significant influence on the response of a laminate to impact and that improvements in damage tolerance are not necessarily made at the expense of laminate room temperature mechanical properties. Neat resin ultimate tensile strengths of greater than 69 MPa and strains at failure of greater than 4 percent were common to most materials that exhibited significant improvements. However, very high resin failure strains were not found to guarantee additional improvements. To ensure adequate laminate compression strength the resin should have a tensile modulus greater than 3.1 GPa and a shear modulus sufficiently high to prevent microbuckling. In addition to adequate tensile strain capability, there must be sufficient resin between the fibers in the laminate to permit plastic deformation of the resin. Preliminary results indicate a resin volume fraction on the order of 40 percent or greater may be necessary to ensure damage tolerance.

The newly developed multi-span beam shear test produced results which correlate well with damage tolerance trends from impact tests. The displacement at first interlaminar fracture for the five systems that demonstrated the highest damage tolerance was approximately twice that of the baseline material. This result is in sharp contrast to results reported for shear strengths based on short beam shear tests. The baseline material had the highest short beam shear strength but the lowest damage tolerance of any material evaluated.

The large number of materials studied and the parameters considered did not permit extensive property evaluation or a large number of replicate tests. Therefore, the results reported should be considered preliminary. The trends observed, however, can form the foundation for future investigations directed toward improving composite damage tolerance.

REFERENCES

1. Rhodes, Marvin D.; Williams, Jerry G.; and Starnes, James H.: Effect of Low-Velocity Impact Damage on the Compressive Strength of Graphite-Epoxy Hat-Stiffened Panels. NASA TN D-8411, 1977.

2. Starnes, James H., Jr.; Rhodes, Marvin D.; and Williams, Jerry G.: The Effect of Impact Damage and Circular Holes on the Compressive Strength of a Graphite-Epoxy Laminate, ASTM STP 696, 1979, pp. 145-171.

3. McGarry, F. J.; and Willner, A.: Toughening of an Epoxy Resin by an Elastomeric Second Phase. Massachusetts Institute of Technology, R68-6, March 1969.

4. Rowe, E. H.: Fractography of Thermoset Resins Toughened With Hycar CTBN. 26th Annual Technical Conference Reinforced Plastics/Composites Division, The Society of the Plastics, Inc. 1971, Section 12-E, pp. 1-7.

5. Perry, J. L.; Kirkhart, J. L.; and Adams, D. F.: Third Phase Fiber Addition to Advanced Graphite Composites for Improvement of Impact Strength. Philco-Ford Corporation, Final Report Navy Contract N00019-73-C-0389, March 1974.

6. Allred, R. E.; Street, H. K.; and Martinez, R. J.: Improvement of Transverse Composite Strength-Test Specimens and Materials Development. SAMPE 24th National Symposium 1979, pp. 31-50.

7. Furney, Michael F.: Rubber-Modified, Low-Density Encapsulant. SAMPE Materials Review 75, Proceedings of 7th National Technical Conference, Albuqurque, NM, October 14-16, 1975, pp. 386-394.

8. Byers, Bruce A.: Behavior of Damaged Graphite-Epoxy Laminates Under Compression Loading. NASA CR 159293, August 1980.

9. Palmer, R. J.: Investigation of the Effect of Resin Material On Impact Damage to Graphite-Epoxy Composites. NASA CR 165677, March 1981.

10. Williams, Jerry G.; Anderson, Melvin S.; Rhodes, Marvin D.; Starnes, James H., Jr.; and Stroud, W. Jefferson: Recent Developments in the Design, Testing, and Impact-Damage Tolerance of Stiffened Composite Panels. Fibrous Composites in Structural Design (Proceedings of Fourth Conference on Fibrous Composites in Structural Design), Plenum Press, 1980, pp. 259-291.

11. Greszczuk, L. B.: Microbuckling Failure of Circular Fiber Reinforced Composites. AIAA/ASME/SAE 15th Structures, Structural Dynamics and Materials Conference, AIAA Paper 74-354, April 17-19, 1974.

12. Rhodes, Marvin D.; Williams, Jerry G.; and Starnes, James H., Jr.: Low-Velocity Impact Damage In Graphite-Fiber Reinforced Epoxy Laminates. Paper presented 34th Annual Conference Reinforced Plastic/Composite Institute, The Society of the Plastics Industry, Inc., New Orleans, LA, January 29-February 2, 1979.

13. Hertzberg, P. E.; Smith, B. W.; and Miller, A. G.: Effect of Matrix Resin on the Impact Fracture Characteristics of Graphite-Epoxy Laminates. NASA CR-165784, 1981.

14. ASTM D-2344-76. Apparent Interlaminar Shear Strength of Parallel Fiber Composites by Short Beam Method. Annual Book of ASTM Standards, Part 36, 1981.

15. Miller, A. G.; Hertzberg, P. E.; and Rantala, V. W.: Toughness Testing of Composite Materials. SAMPE Quarterly, January 1981, pp. 36-42.

16. Bascom, W.D.; Bitner, J. L.; Moulton R.J.; and Siebert, A. R.: The Interlaminar Fracture of Organic-Matrix Woven Reinforcement Composites. Composites, January 1980, pp. 9-18.

17. Rhodes, Marvin D.: Damage Tolerance Research on Composite Compression Panels. NASA Conference Publication 2142, 1980, pp. 107-142.

18. Rhodes, Marvin D.; and Williams, Jerry G.: Concepts for Improving the Damage Tolerance of Composite Compression Panels. Paper presented at 5th DOD/NASA Conference on Fibrous Composites In Structural Design. New Orleans, LA, January 27-29, 1981.

TABLE I.- RESIN MATERIALS

MATERIAL	SUPPLIER	RESIN IDENTIFICATION	RESIN GENERIC CHEMISTRY	NEAT RESIN PROPERTIES			CURE TEMPERATURE, °C
				TENSILE ULTIMATE, MPa	TENSILE MODULUS, GPa	PERCENT ELONGATION AT FAILURE	
1[a]	Narmco	5208	MY-720+ Aromatic Amine	57	4.0	1.5	177
2	Air Logistics	X-1	Bisphenol Epoxy + Amine + Elastomer	48	1.7	8.0	149
3	American Cyanamid	BP-907	Bisphenol A Epoxy + Latent Aliphatic Amine + Vinyl Resin Modifier	90	3.1	4.8	177
4	American Cyanamid	919	Bisphenol A/Epoxy Novalac + Latent Aliphatic Amine + Elastomers	n.a.[b]	n.a.	n.a.	177
5	American Cyanamid	937	Bisphenol A + Specialty Latent Aromatic and Aliphatic Amines + Elastomers	n.a.	n.a.	n.a.	177
6	American Cyanamid	982	Bisphenol A/Epoxy Novalac + Latent Aromatic and Aliphatic Amines	n.a.	n.a.	n.a.	177
7	Ciba Geigy	X-1	Hydantoin Epoxy + Aromatic Amine	99	4.4	8.7	177
8	Ciba Geigy	X-1M	Hydantoin Epoxy + Aromatic Amine + Thermoplastic	n.a.	n.a.	n.a.	177
9	Ciba Geigy	X-2	Hydantoin Epoxy + Aromatic Amine	103	3.3	7.0	149
10	Ciba Geigy	X-3	Hydantoin Epoxy + Aromatic Amine	94	3.3	7.0	177
11	Ciba Geigy	X-4	Bisphenol A Epoxy + Aliphatic Amine + Thermoplastic	90	3.3	4.6	121
12	Ciba Geigy	Fiberdux 920	Bisphenol A Epoxy + Aliphatic Amine + Thermoplastic	75	3.1	4.1	121
13	Ciba Geigy	Fiberdux 914	Multifunctional Epoxy + Thermoplastic	50	4.0	1.4	204
14	Fiberite	HY-E 976	High Functionality Epoxy + Aromatic Amine	62	2.8	5.0	177
15	Hexcel	X-1	Bisphenol A Epoxy + High Functionality Epoxy + Dicyanamide + Elastomer	53	2.2	7.0	121
16	Hexcel	X-2	Bisphenol A and Epoxies + Dicyanamide + Elastomer	45	2.6	1.9	177
17	Hexcel	X-TR1	Bisphenol A Epoxy + Dicyanamide + Elastomers	n.a.	n.a.	n.a.	121
18	Narmco	95995	Epoxy + Aromatic Amine	74	3.7	2.4	177
19	Narmco	X1114	Bisphenol A Epoxy + Non-aromatic Amine + Elastomers	31	1.7	6.0	121
20	Narmco	X108/34A	Bisphenol A Epoxy + Aromatic Amine + Elastomers	n.a.	n.a.	n.a.	177
21	Narmco	X-107	Bisphenol A Epoxy + Non-aromatic Amine + Elastomers	n.a.	n.a.	n.a.	177
22	Narmco	X-109	Bisphenol A Epoxy + Non aromatic Amine + Elastomers	n.a.	n.a.	n.a.	177
23	U.S. Polymeric	X-1	Bisphenol A Epoxy + Specialty Aromatic Amine + Elastomers	48	2.3	19.0	177
24	U.S. Polymeric	X-2	Bisphenol A Epoxy + Specialty Aromatic Amine + Elastomers	94	n.a.	8.0	149

[a] Baseline material
[b] n.a. - not available

TABLE II.- UNIDIRECTIONAL COMPOSITE MATERIAL PROPERTIES

Material	Resin Mass Percent	Tension		Compression		Short Beam Shear Strength MPa
		Strength, GPa	Modulus, GPa	Strength, Pa	Modulus, GPa	
1	28.0	1.50	131	1.45	124	131
2	27.0	1.64	115	.61	108	57
3	31.7	1.70	130	1.23	112	103
4	31.7	1.79	142	1.34	128	103
5	31.7	1.71	144	1.52	123	108
6	27.0	1.68	143	1.78	119	115
7	25.7	2.25	155	1.56	145	90
8	27.6	1.94	157	1.63	122	72
9	25.0	1.91	148	1.02	132	63
10	23.4	2.14	152	1.48	138	85
11	28.7	1.92	124	1.14	138	112
12	33.5	1.94	142	1.15	123	97
13	n.a.	1.86	143	1.60	121	124
14	n.a.	1.59	128	1.10	117	121
15	28.8	1.88	141	0.80	121	89
16	28.9	1.70	131	1.05	120	93
17	n.a.[a]	n.a.	n.a.	n.a.	n.a.	n.a.
18	33.0	1.40	114	1.31	103	125
19	30.8	1.73	146	.48	107	54
20	24.0	1.77	145	1.07	134	135
21	29.8	1.60	136	.75	121	93
22	33.5	1.68	132	.65	115	84
23	24.6	1.84	134	.64	136	84
24	24.8	2.12	165	1.63	134	109

a n.a. - not available

TABLE III.- IMPACT DAMAGE MEASUREMENTS

Material	Specimen Thickness, mm	Impact Velocity m/s	C-scan Damage Area, cm	Length of Visible Back Surface Damage
1	6.25	112	26.9	6.35
2	7.92	106	6.1	NONE
3	7.80	106	6.4	0.51
	6.80	105	5.2	0.51
4	6.78	109	9.5	2.54
5	6.86	114	9.1	NONE
6	6.60	110	15.8	5.59
7	6.35	108	12.6	3.30
8	7.24	109	20.5	n.a.
	6.22	104	n.a.[a]	n.a.
9	6.22	108	17.8	4.06
10	6.65	108	16.5	1.27
11	9.30	105	9.8	NONE
	7.62	103	10.2	NONE
12	7.11	108	n.a.	NONE
	6.35	106	6.1	NONE
13	5.89	n.a.	n.a.	n.a.
14	6.86	109	14.8	6.35
15	6.68	104	5.5	NONE
16	7.19	108	n.a.	NONE
17	7.67	91	3.1	n.a.
18	7.87	88	19.4	3.05
19	8.08	105	2.4	NONE
	7.24	104	5.7	NONE
20	6.22	109	16.1	4.83
21	8.08	104	12.7	NONE
22	7.54	101	5.4	NONE
23	6.30	105	7.5	2.03
24	5.97	107	16.1	2.03

a n.a. - not available

TABLE IV.- MULTI-SPAN BEAM SHEAR TEST RESULTS

Material	Specimen Thickness, mm	First Failure		Maximum	
		Normalized Load[a]	Normalized Displacement[b]	Normalized Load[a]	Normalized Displacement[b]
1	6.38	1.00	1.00	c	c
2	7.80	1.11	1.79	c	c
3	6.71	1.81	2.06	c	c
4	6.71	1.54	1.79	c	c
5	6.73	1.49	1.78	c	c
6	6.55	.86	.92	1.39	1.65
7	6.58	1.09	1.22	c	c
8	7.11	.99	.94	1.06	1.06
9	5.99	1.56	1.51	c	c
10	6.93	1.20	1.46	c	c
11	7.16	1.95	2.11	c	c
12	7.06	1.91	2.75	c	c
	6.30	1.64	1.97	c	c
14	6.76	1.06	1.08	1.11	1.33
15	6.65	1.49	1.90	c	c
16	7.29	1.71	2.39	c	c
17	7.70	n.a.	n.a.	1.51	3.21
18	7.39	1.37	1.33	1.40	1.47
19	8.18	n.a.[d]	n.a.	1.94	4.13
	7.59	n.a.	n.a.	1.69	3.76
20	6.38	1.52	1.56	c	c
21	7.77	1.76	2.25	c	c
22	7.75	1.73	2.43	c	c
23	6.20	1.19	1.82	c	c
24	6.02	1.05	1.16	c	c

[a] Normalized by value of 23.3 kN. Recorded at first failure for material 1.
[b] Normalized by value of 0.38 mm. Recorded at first failure for material 1.
[c] First failure value was the maximum recorded during test.
[d] n.a. - not available.

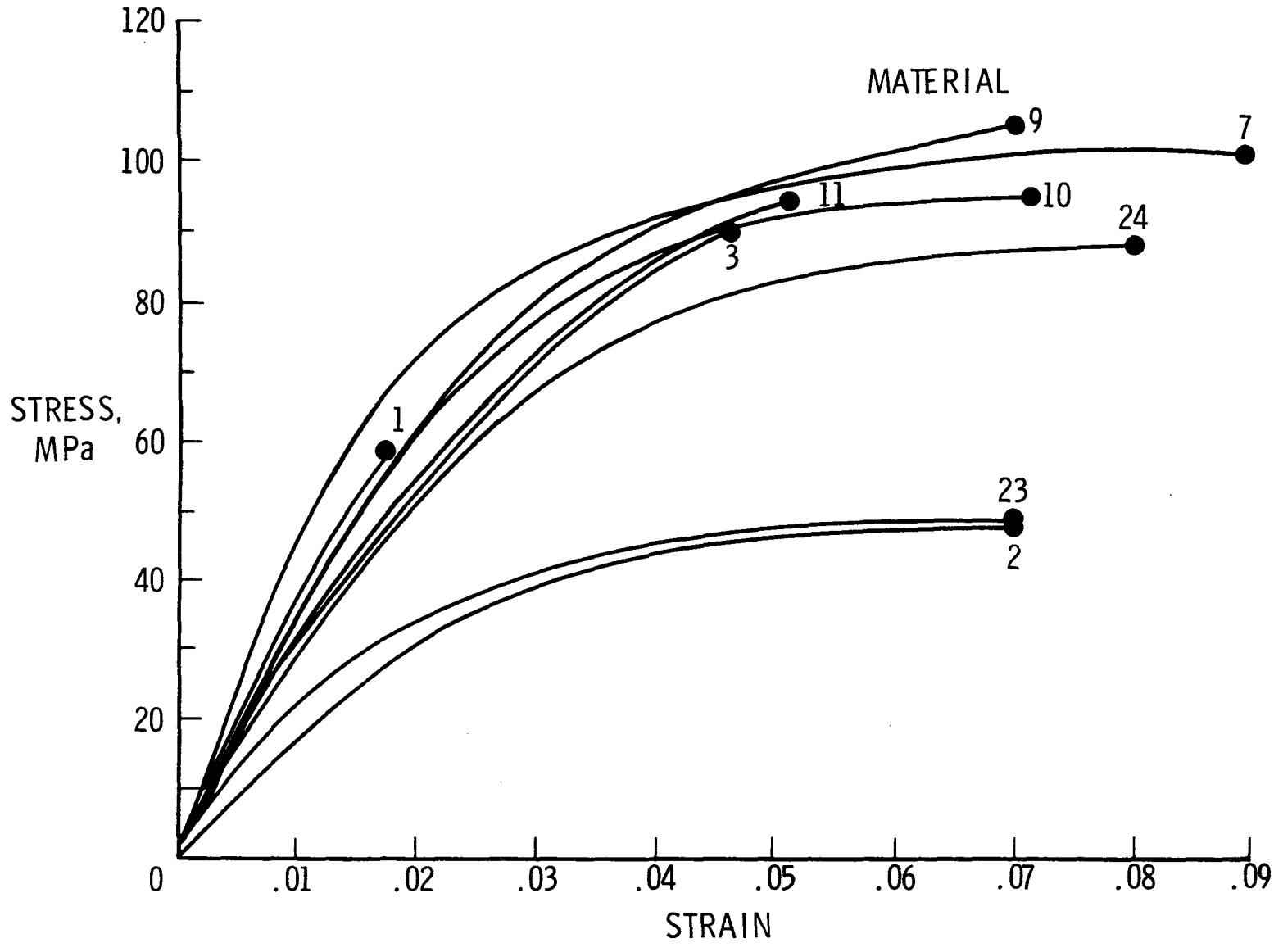

Figure 1.- Neat resin tension stress-strain curves.

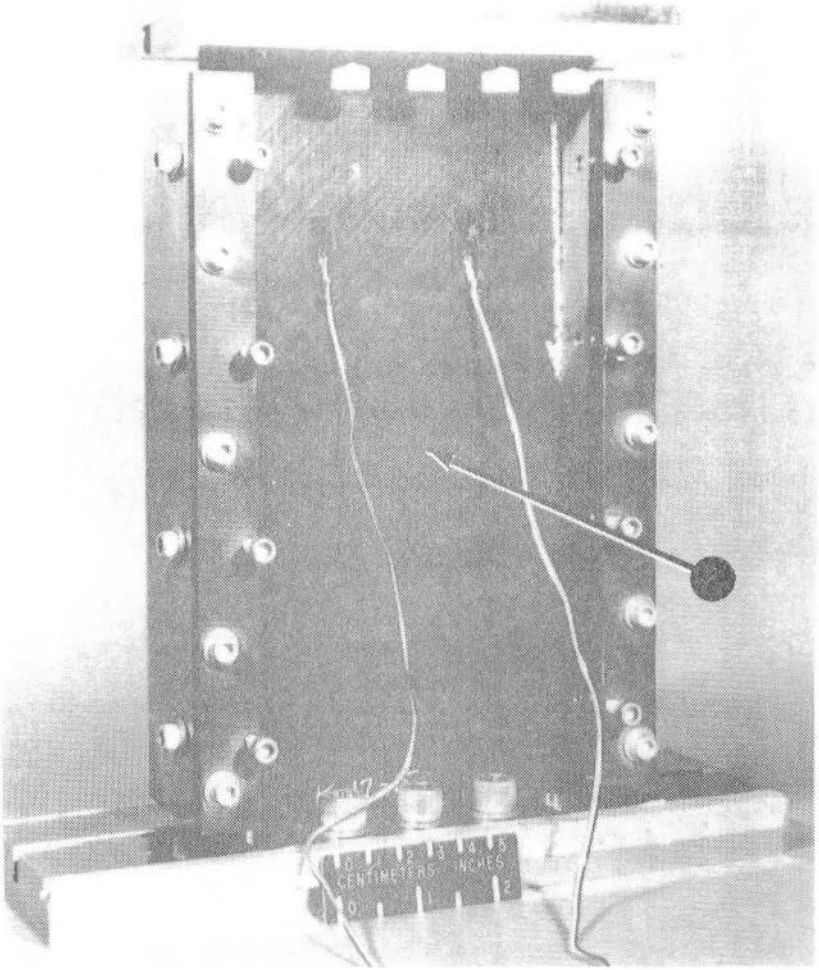

(a) Impact under compression load.

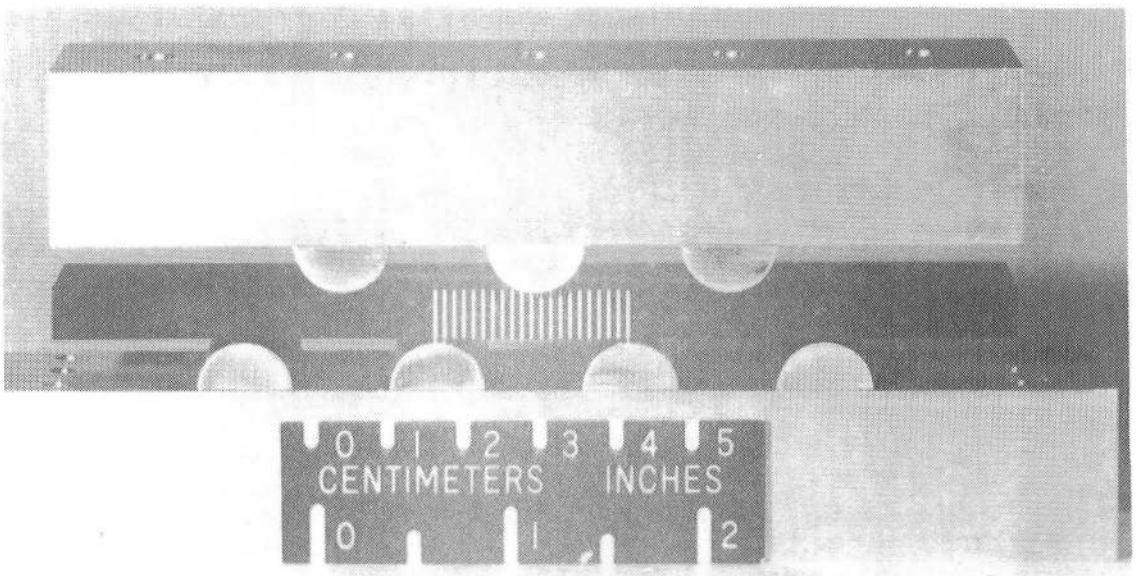

(b) Multi-span beam shear.

Figure 2.- Test apparatus and specimen.

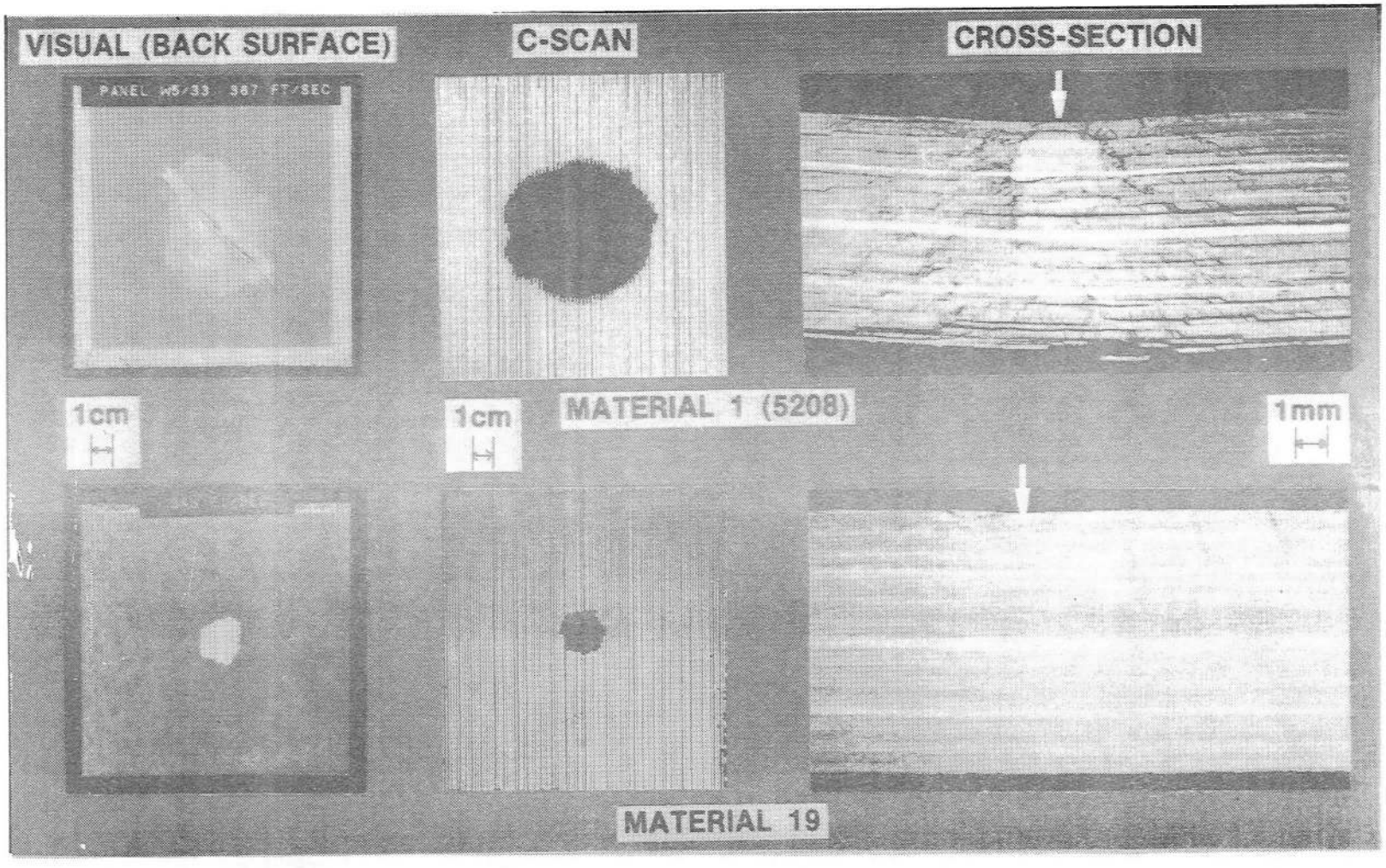

Figure 3.- Damage in 48-ply laminates due to impact by 1.27 cm diameter aluminum sphere impacting at approximately 110 m/s. Arrow denotes impact location.

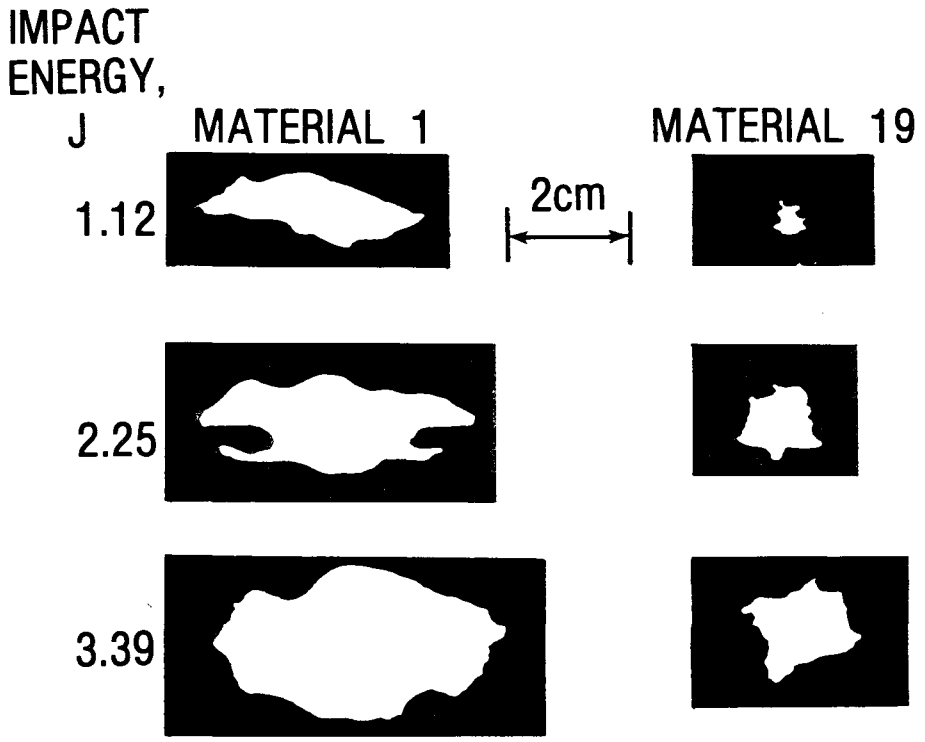

(a) C-scan comparison.

Figure 4.- C-scan damage resulting from Gardner impact test.

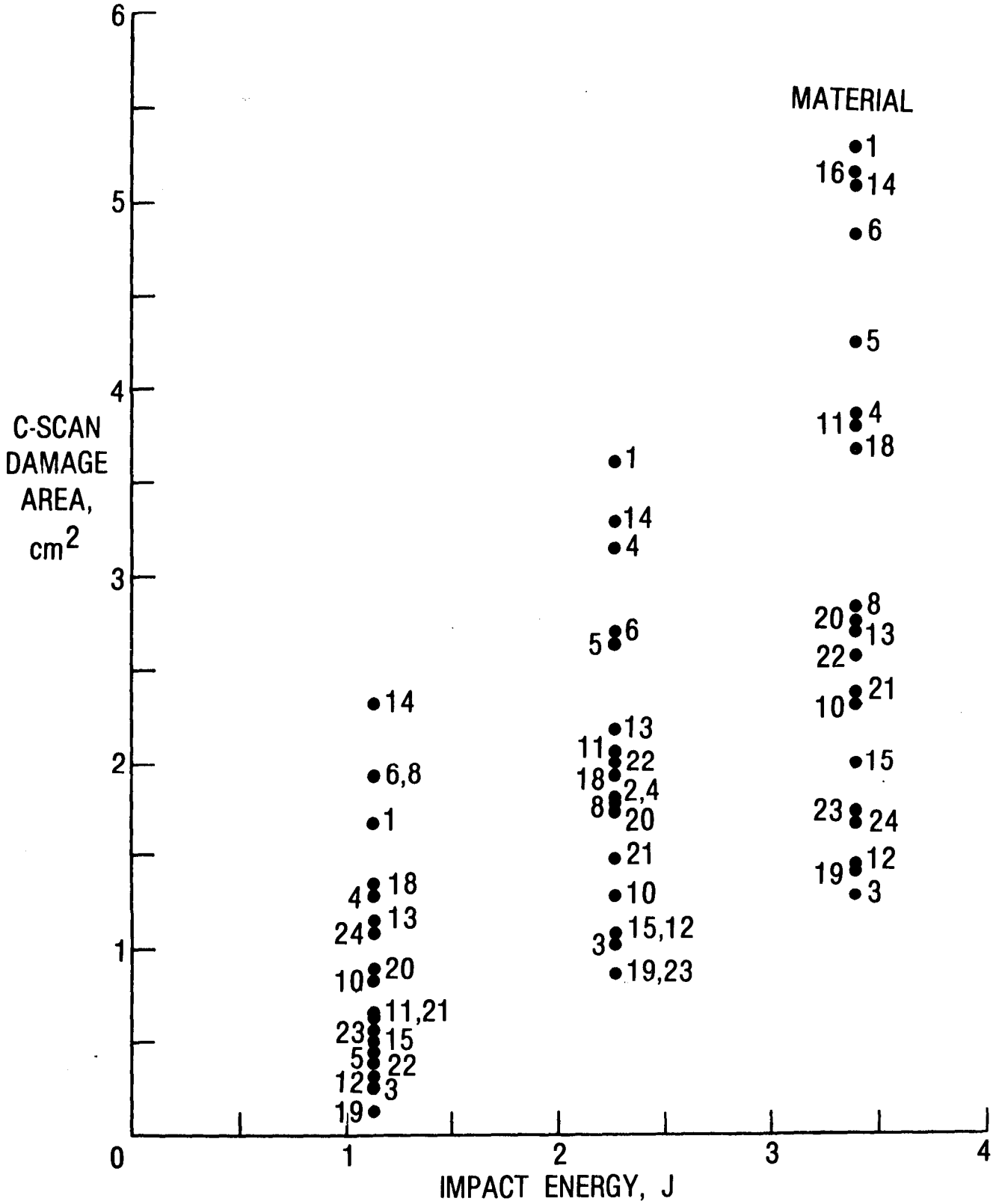

(b) Damage area comparison.

Figure 4.- Concluded.

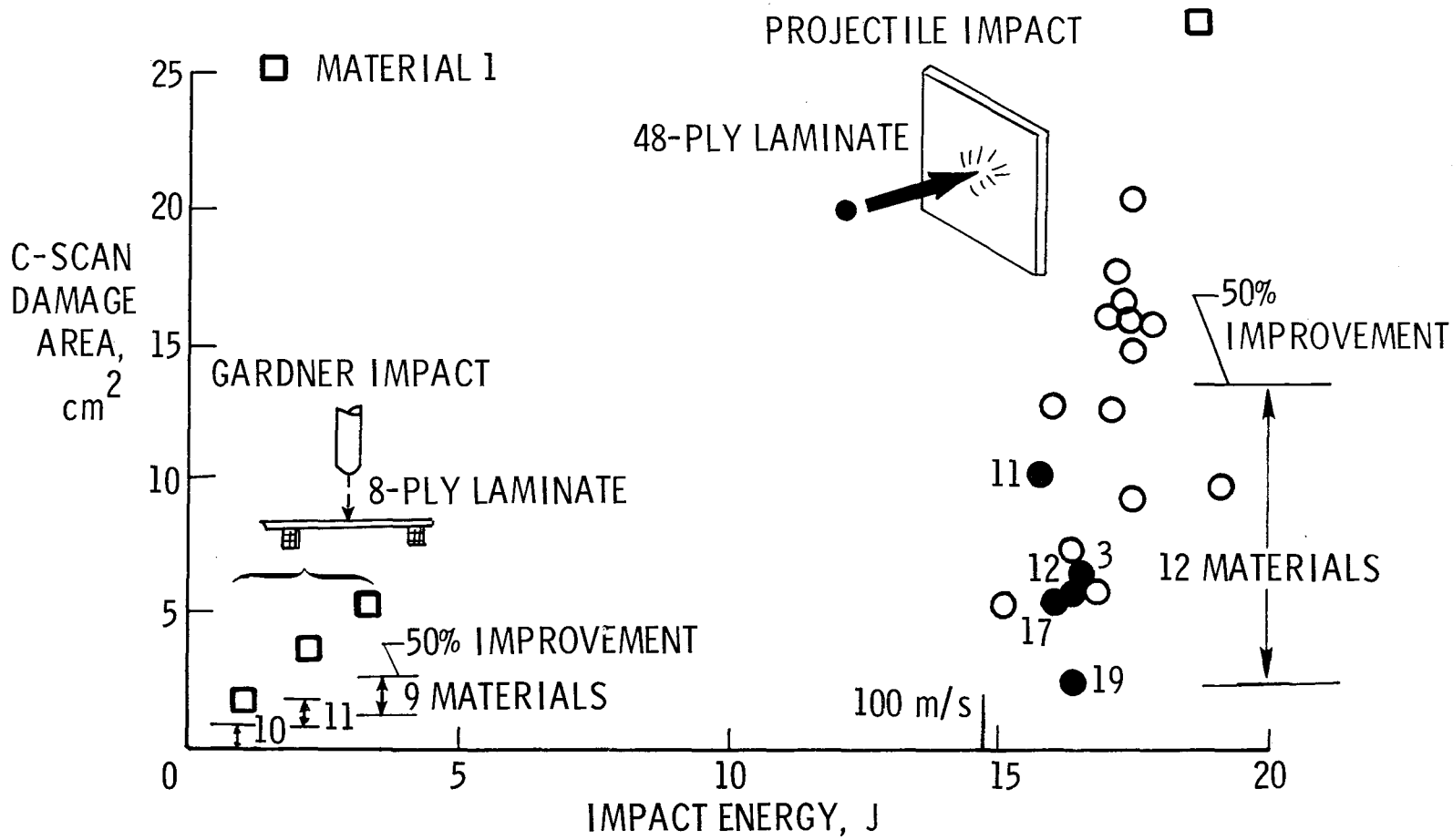

Figure 5.- Impact damage area resulting from Gardner and projectile impact tests.

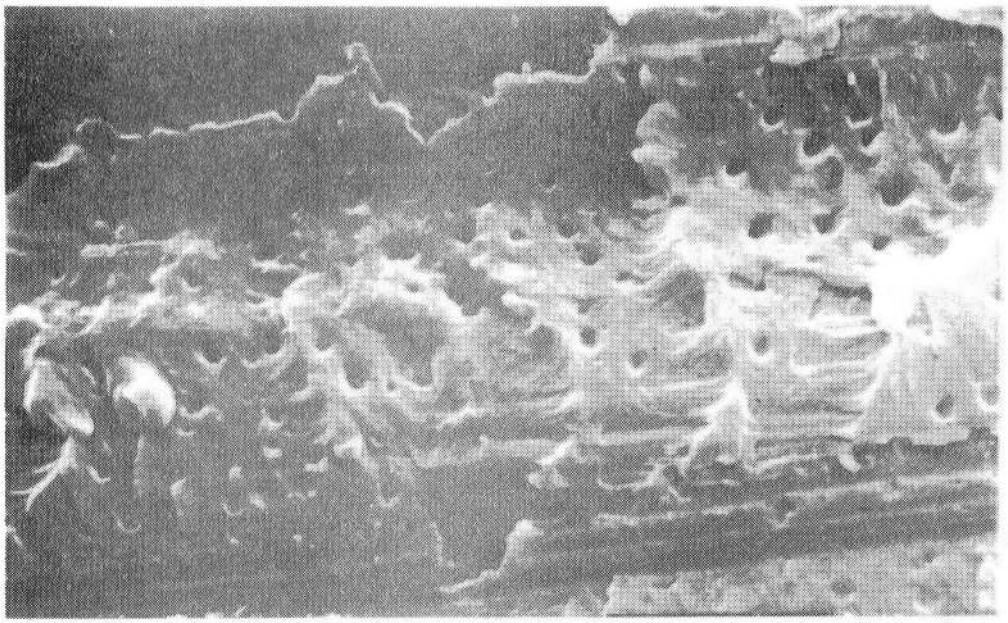

(a) "Pits" in fracture surface (material 15).

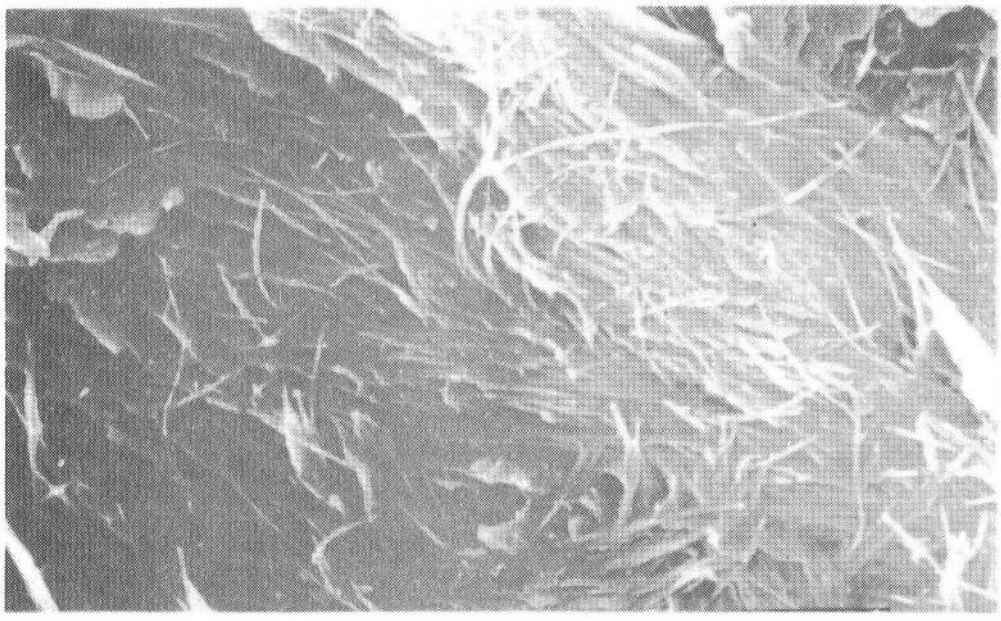

(b) "Hairs" in fracture surface (material 21).

Figure 6.- Typical fracture surfaces for elastomer modified resin systems.

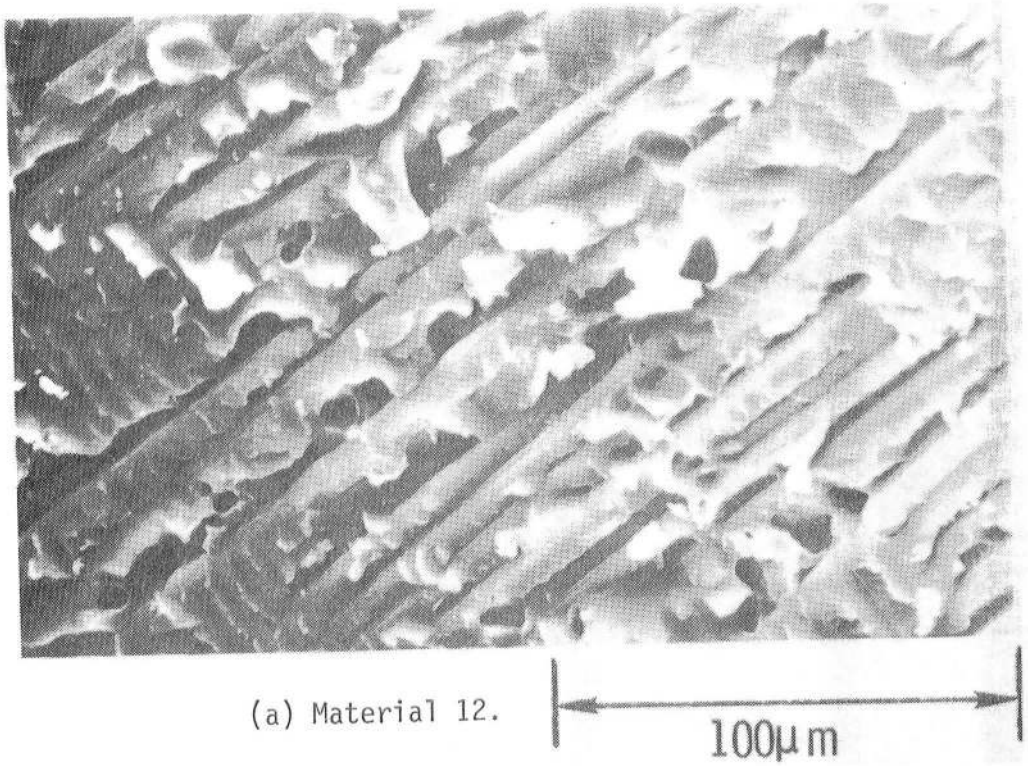

(a) Material 12.

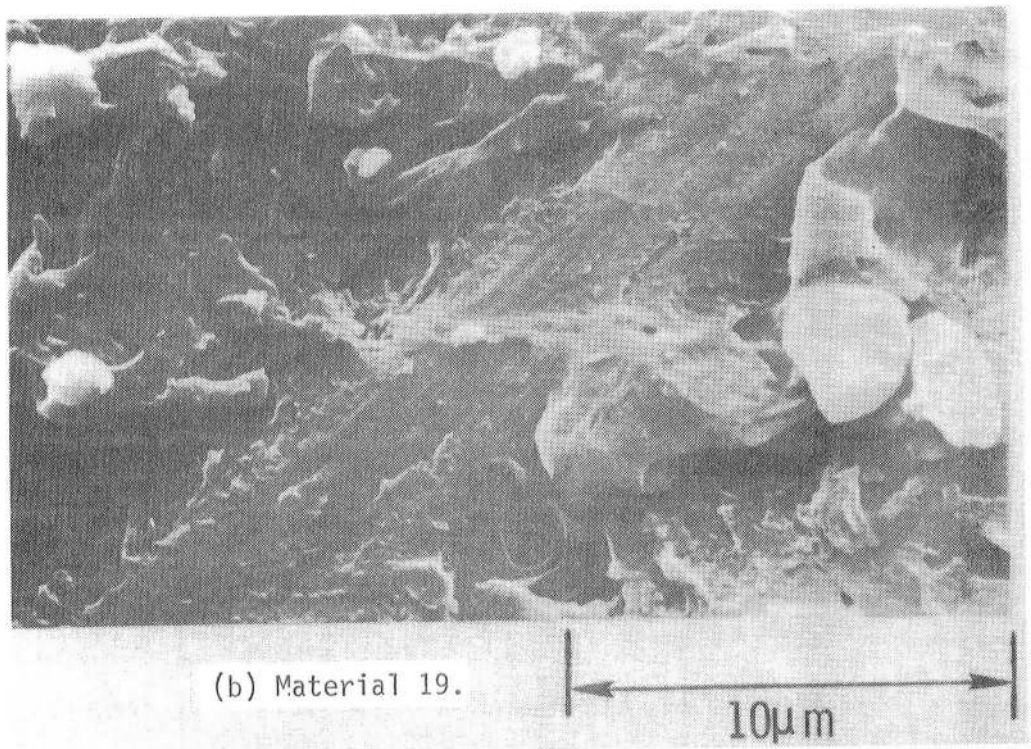

(b) Material 19.

Figure 7.- Hackly appearance in failure surface of laminates constructed with ductile resin systems.

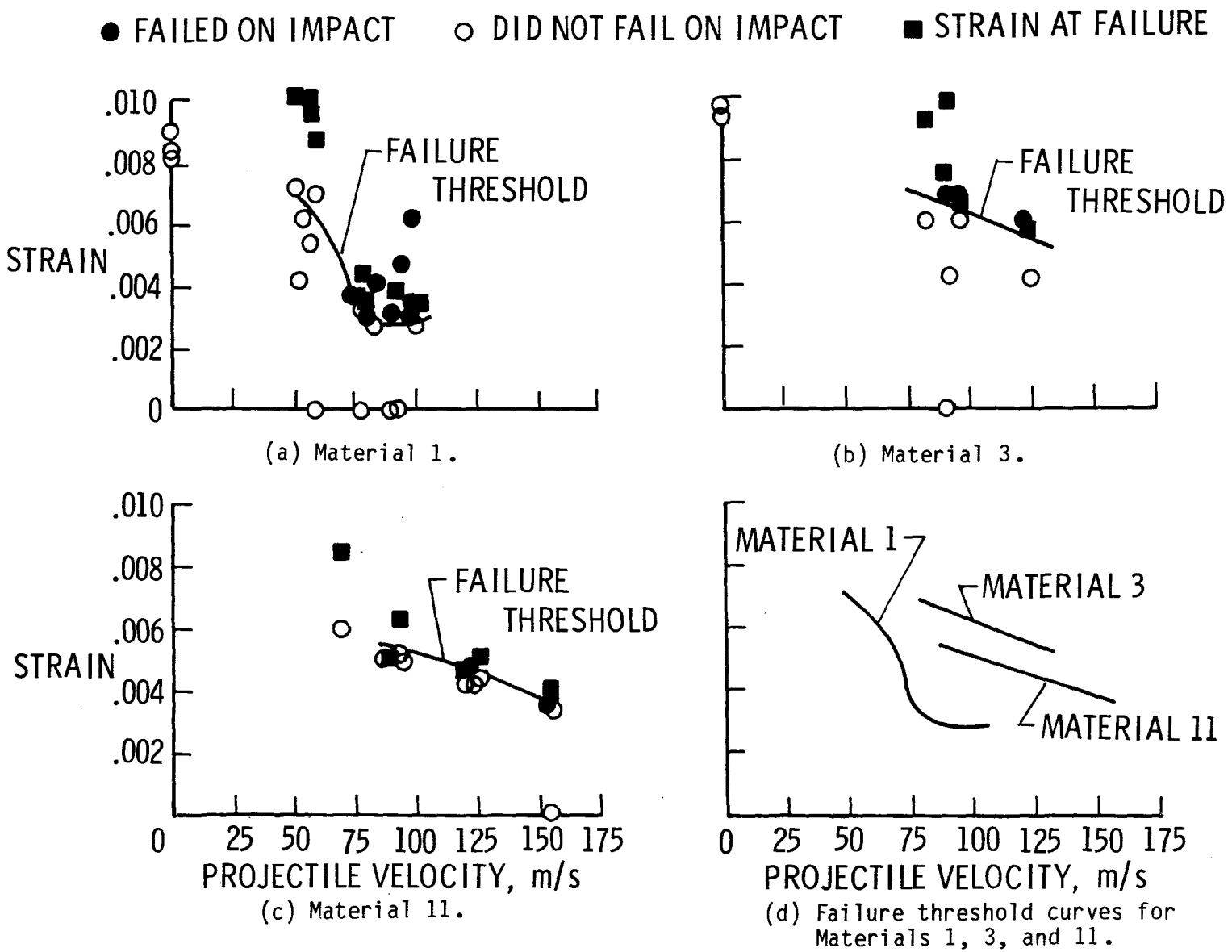

Figure 8.- Effect of impact damage on the compression failure strain of three of the resin material systems.

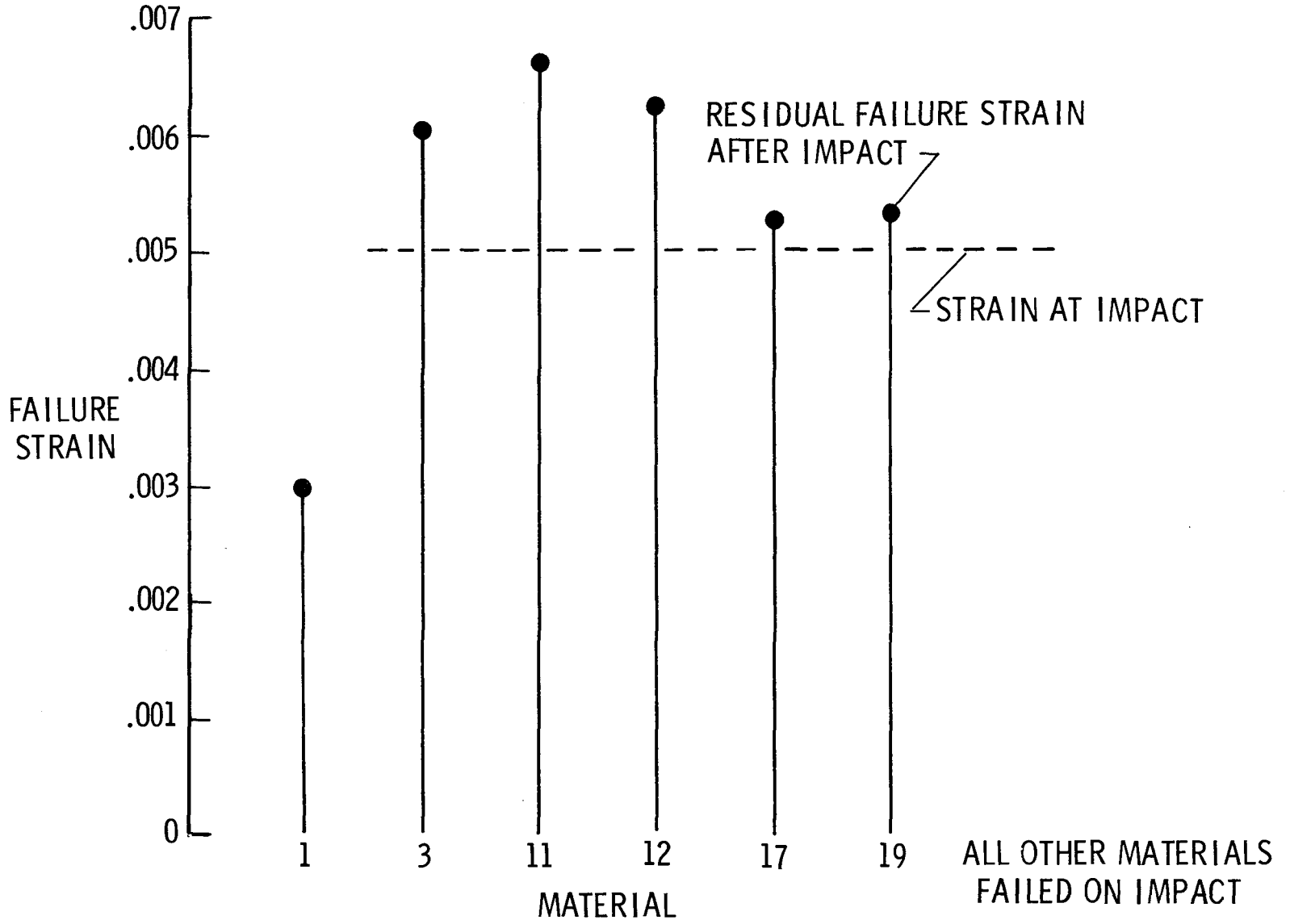

Figure 9.- Loaded impact screening test results.

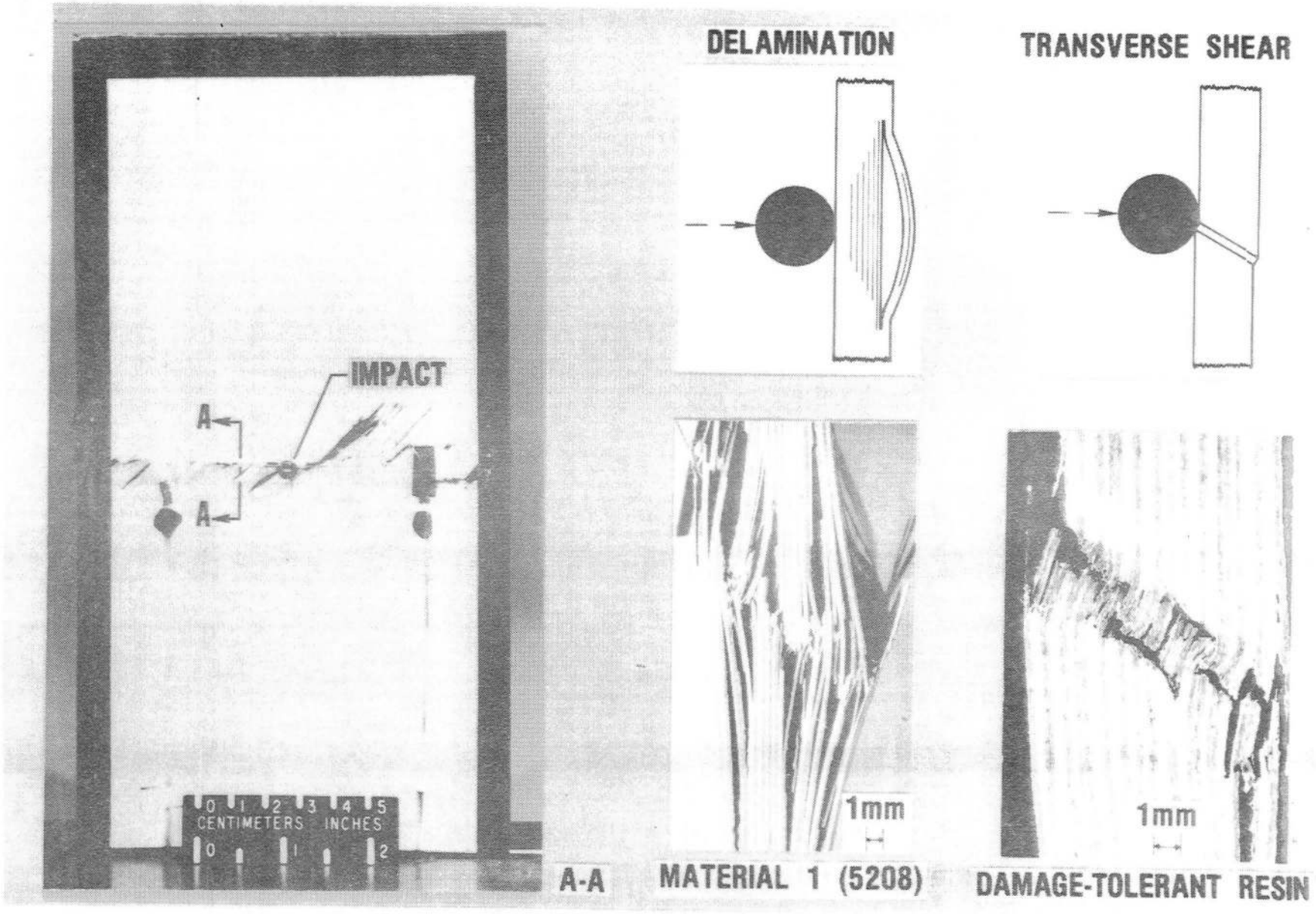

Figure 10.- Failure propagation modes due to impact initiated damage.

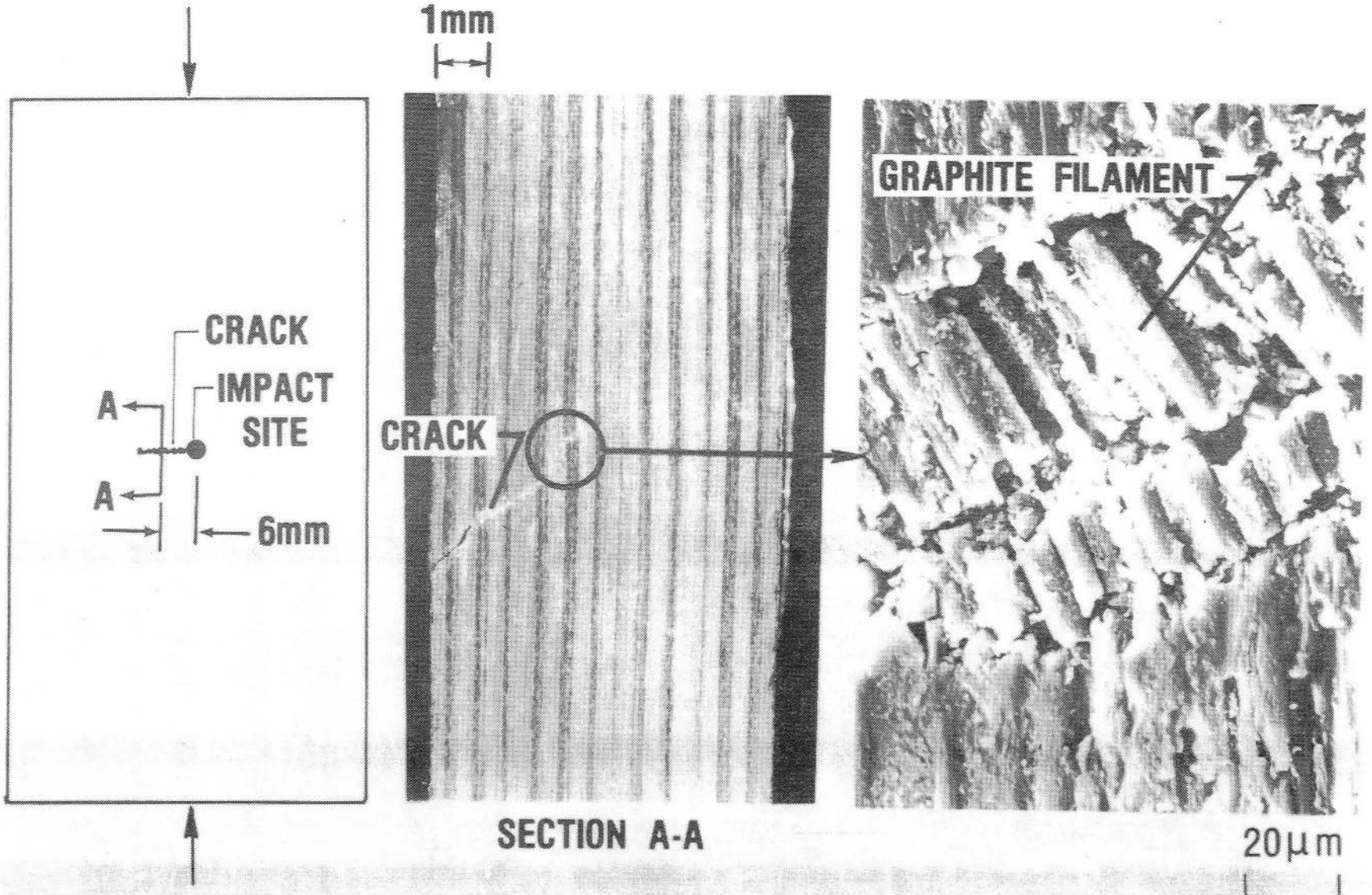

Figure 11.- Transverse shear failure observed in cross section of material 17.

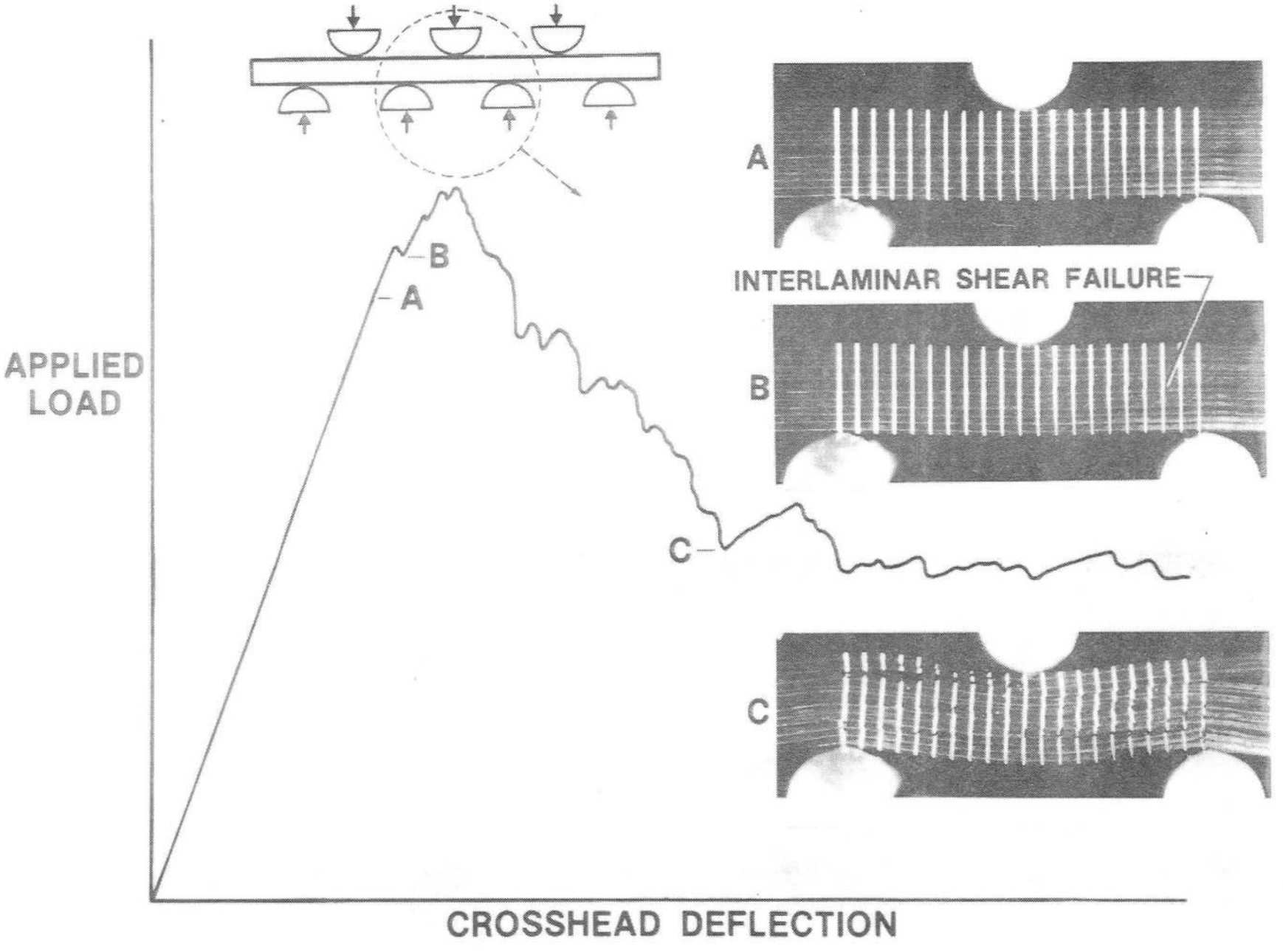

Figure 12.- Load-deflection response and associated failure mode for a typical multi-span beam shear test specimen.

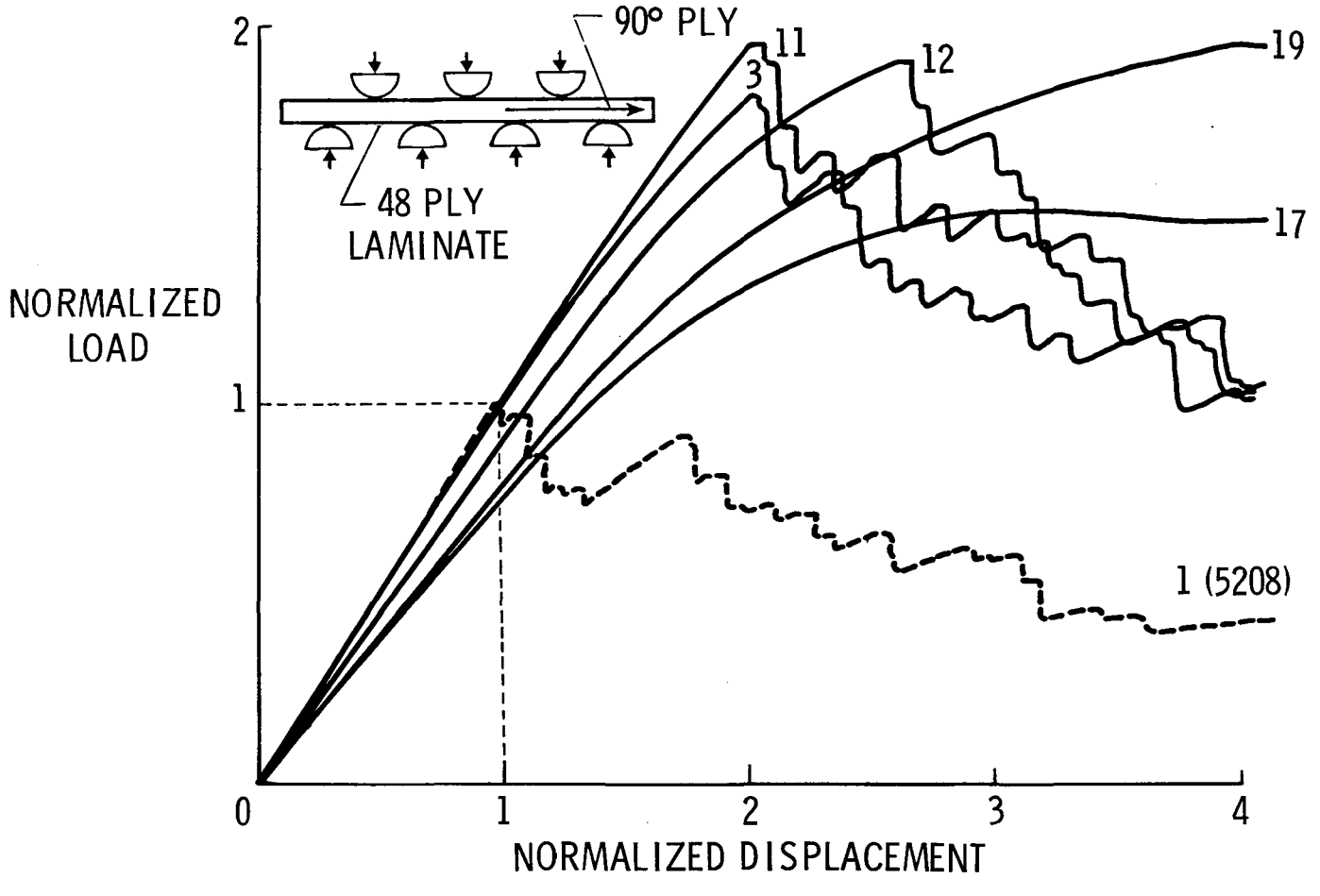

Figure 13.- Comparison of multi-span beam shear load-displacement response for six material systems.

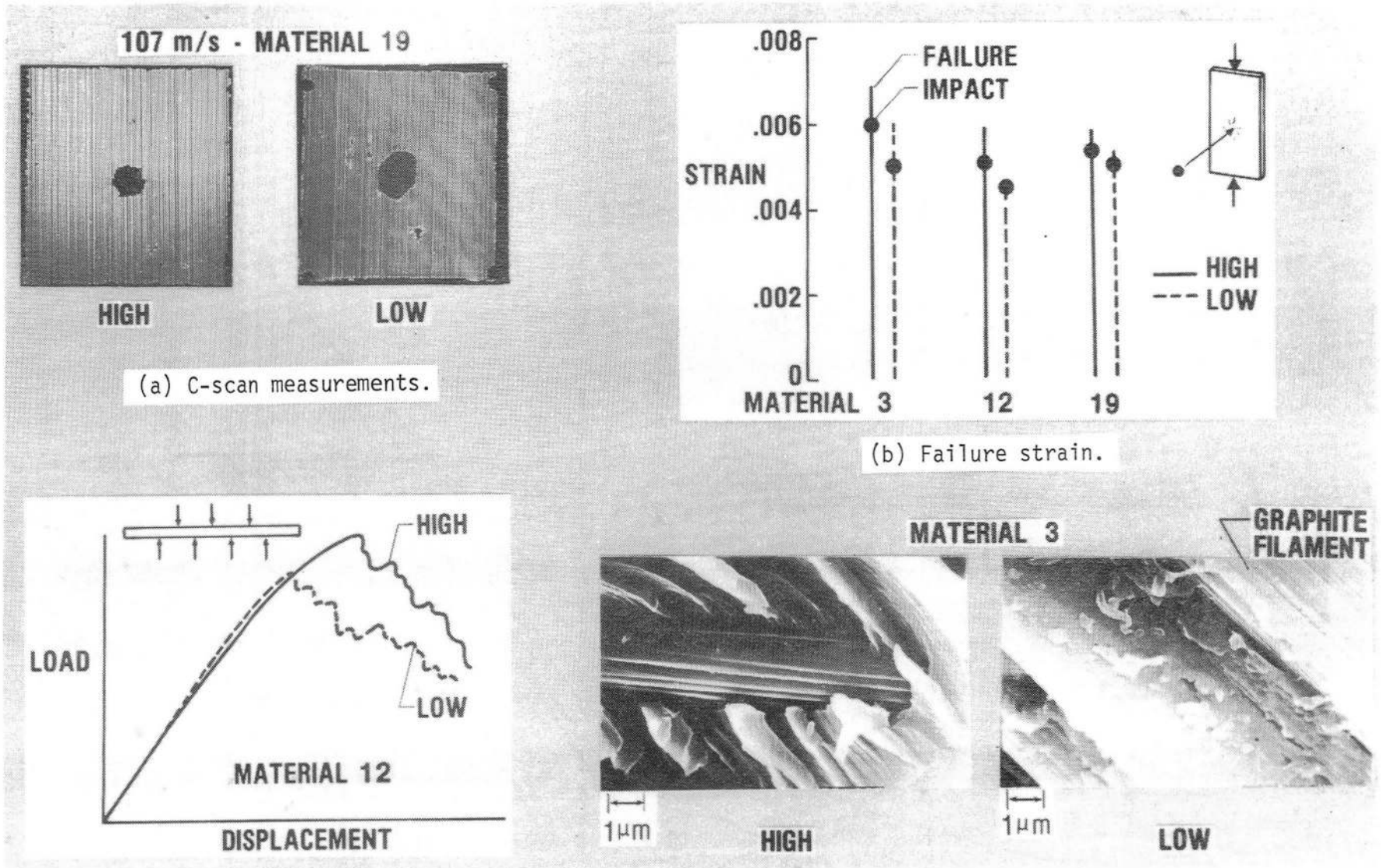

Figure 14.- Effect of resin volume fraction on composite laminate damage tolerance characteristics.

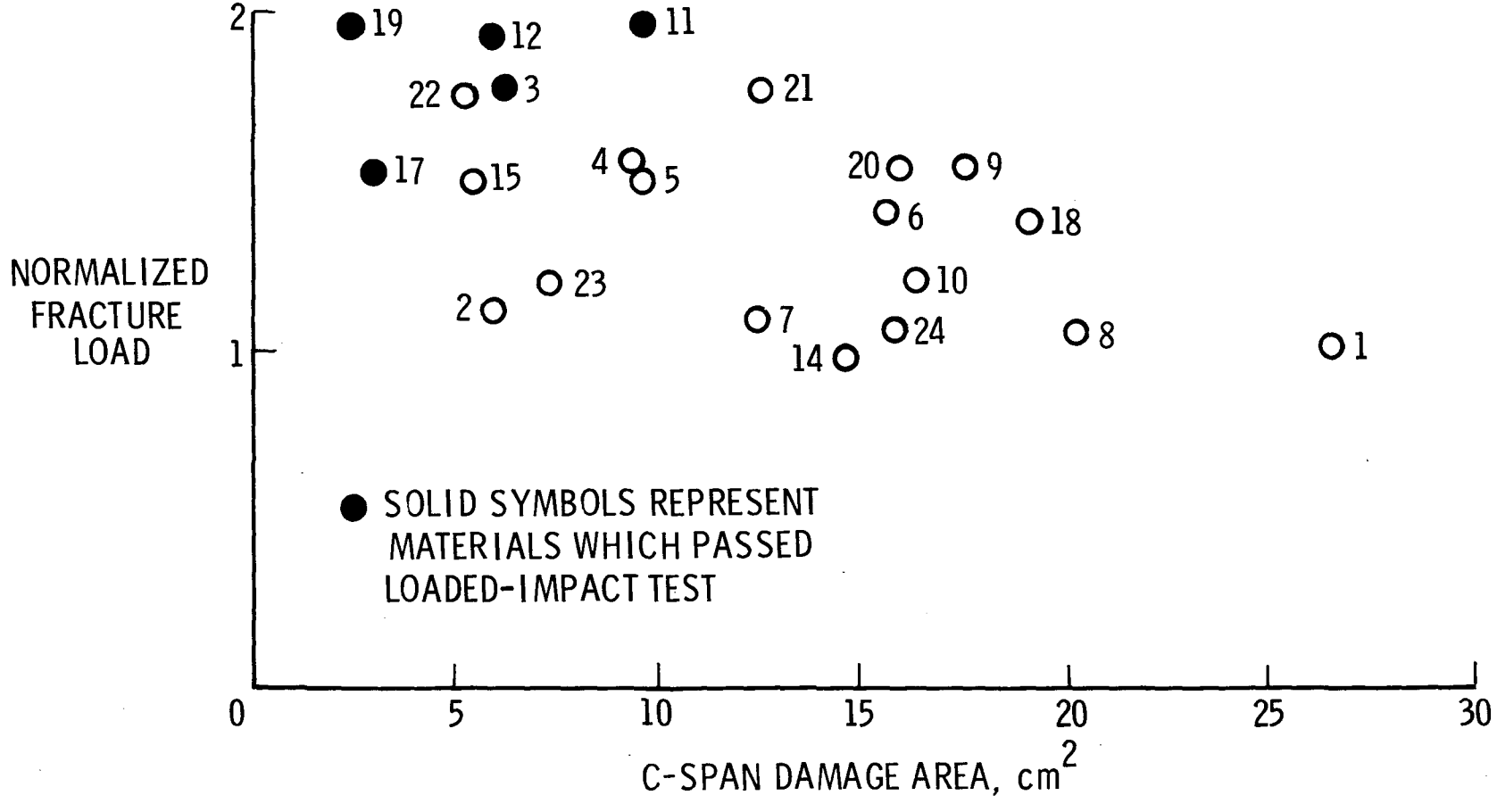

Figure 15.- Comparison of C-scan damage area due to projectile impact and load at first interlaminar fracture from multi-span beam shear test for several material systems.

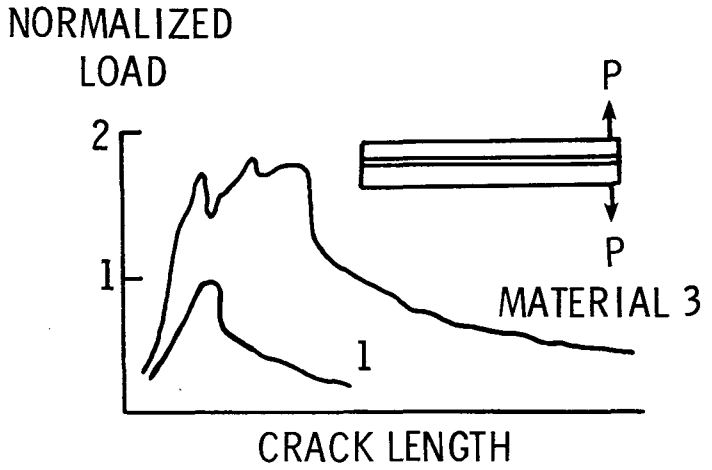

Figure 16.- Double-cantilever beam test results for two material systems.

1. Report No.	2. Government Accession No.	3. Recipient's Catalog No.
NASA TM-83213		

4. Title and Subtitle	5. Report Date
The Effect of Resin On the Impact Damage Tolerance of Graphite-Epoxy Laminates	October 1981
	6. Performing Organization Code: 505-33-33-06
7. Author(s): Jerry G. Williams and Marvin D. Rhodes	8. Performing Organization Report No.
	10. Work Unit No.
9. Performing Organization Name and Address: NASA Langley Research Center, Hampton, VA 23665	11. Contract or Grant No.
	13. Type of Report and Period Covered: Technical Memorandum
12. Sponsoring Agency Name and Address: National Aeronautics and Space Administration, Washington, DC 20546	14. Sponsoring Agency Code

15. Supplementary Notes

Paper presented at ASTM Sixth Conference On Composite Materials: Testing and Design. Phoenix, AZ, May 1981.

16. Abstract

An experimental investigation was conducted to evaluate the effect of the matrix resin on the impact damage tolerance of graphite-epoxy composite laminates. The materials were evaluated on the basis of the damage incurred due to local impact and on their ability to retain compression strength in the presence of impact damage. Twenty-four different resin systems supplied by seven manufacturers in prepreg tape form were evaluated. Materials were not competitively submitted for the purpose of selecting a best material but were voluntarily provided to study what improvements in damage tolerance the various resin improvements might make. Most of the materials tested had a smaller interior damage region as determined by C-scan inspection and less damage on the specimen surface than a baseline control resin which is widely used and whose damage tolerance characteristics have been documented. Five of the systems demonstrated substantial improvements compared to the baseline system including retention of compression strength in the presence of impact damage. Examination of the neat resin mechanical properties indicates the resin tensile properties influence significantly the laminate damage tolerance and that improvements in laminate damage tolerance are not necessarily made at the expense of room temperature mechanical properties. Preliminary results indicate a resin volume fraction on the order of 40 percent or greater may be required to permit the plastic flow between fibers necessary for improved damage tolerance. Test techniques for evaluating damage tolerance are discussed including a newly developed multi-span beam shear test for which test results correlate well with damage tolerance trends from impact tests.

17. Key Words (Suggested by Author(s))	18. Distribution Statement
Composite Materials Damage Tolerance Epoxy Resins Compression Strength	Unclassified - Unlimited Subject Category 24

19. Security Classif. (of this report)	20. Security Classif. (of this page)	21. No. of Pages	22. Price
Unclassified	Unclassified	45	A03